Chem Catalysis

CellPress

Article

High carbon utilization for CO_2 conversion with chloromethane to aromatics over acidic zeolite catalyst

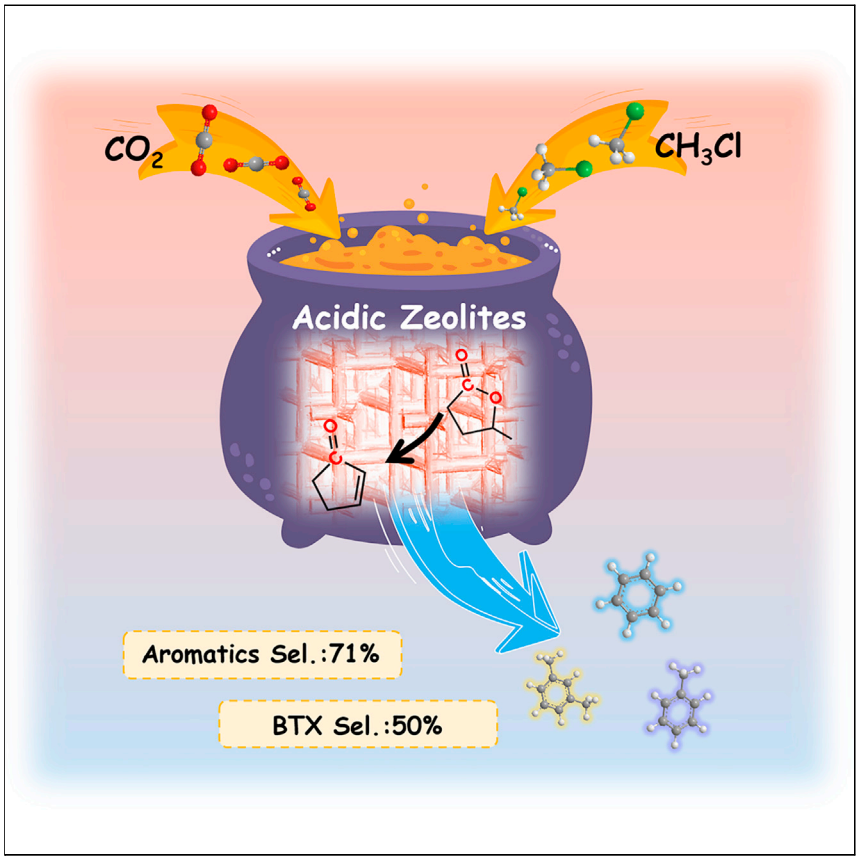

Achieving the conversion of CO_2 and CH_4 to aromatics is a sustainable pathway for reducing greenhouse effects. The key obstacles are the high thermodynamic stability and C–C coupling barriers. Liu's team report a novel route via coupling conversion of CO_2 and CH_3Cl, as an important methane derivative, catalyzed by acidic zeolites, which obtains up to 71% aromatics selectivity with 50% BTX selectivity. Importantly, this work demonstrates that CO_2 directly participates in the formation of aromatics via lactone as key intermediate.

Xudong Fang, Bin Li, Hongchao Liu, ..., Jingfeng Han, Wenliang Zhu, Zhongmin Liu

chliu@dicp.ac.cn (H.L.)
wlzhu@dicp.ac.cn (W.Z.)

Highlights

A novel pathway for utilizing CO_2 and CH_4 has been reported

CO_2 directly participates in producing aromatics, obtaining high carbon utilization

A new aromatization mechanism via lactone and cyclopentene species is clarified

Fang et al., Chem Catalysis 3, 100689
August 17, 2023
https://doi.org/10.1016/j.checat.2023.100689

Please cite this article in press as: Fang et al., High carbon utilization for CO_2 conversion with chloromethane to aromatics over acidic zeolite catalyst, Chem Catalysis (2023), https://doi.org/10.1016/j.checat.2023.100689

Chem Catalysis

CellPress

Article

High carbon utilization for CO_2 conversion with chloromethane to aromatics over acidic zeolite catalyst

Xudong Fang,[1,2] Bin Li,[1,2] Hongchao Liu,[1,*] Mingguan Xie,[1,2] Zhiyang Chen,[1,2] Leilei Yang,[1,2] Jingfeng Han,[1] Wenliang Zhu,[1,3,*] and Zhongmin Liu[1,2]

SUMMARY

Carbon dioxide (CO_2) and methane (CH_4) are major greenhouse gases, and the use of these C1 resources to produce high-value chemicals is significant for sustainable chemistry. Due to the high stability and C–C coupling barriers, simultaneous conversion of CO_2 and CH_4 to aromatics remains challenging. Herein, we report a sustainable strategy for utilizing greenhouse gases based on the conversion of CO_2 and CH_3Cl, an alternative of CH_4, that yields a high aromatics selectivity (71.3%) with ~50% BTX selectivity using H–ZSM–5 as catalyst at 723 K and 3 MPa. *In situ* characterization and ^{13}C isotope-labeling experiments demonstrate that CO_2 directly participates in the formation of aromatics via lactone species instead of undergoing a classical reverse water-gas shift reaction. Furthermore, a unique mechanism for CO_2 conversion is proposed, involving the formation and subsequent transformation of lactone and cyclopentenone species. This work expands high carbon utilization pathways for converting greenhouse gases into chemicals.

THE BIGGER PICTURE

Due to a sharp increase in anthropogenic greenhouse gas emissions and vast natural gas reserves, comprehensively utilizing CO_2 and CH_4 for production of aromatics has been a hot topic in research. However, it remains a challenge owing to the highly thermodynamic stability. Herein, we report a novel strategy on the utilization of greenhouse gases by the coupling of CH_3Cl and CO_2 over H-zeolites with a 10MR. Through this approach, CO_2 can directly participate in the formation of aromatics, resulting in high carbon utilization. This work offers a new concept for the direct coupling of CO_2 with small compounds, which provides a promising and sustainable pathway for utilizing CO_2 and CH_4 for the production of valuable aromatics while reducing greenhouse gas emissions.

INTRODUCTION

Carbon dioxide (CO_2) is a major greenhouse gas, provoking serious environmental problems. In principle, CO_2 is also considered a significant and alternative C1 feedstock since it is inexpensive and substantial.[1,2] Therefore, efficiently utilizing CO_2 to produce high-value chemicals has attracted much attention[1,3,4] but remains a great challenge owing to the inertness of CO_2 ($\Delta_f G^0 = -396$ kJ/mol). Thermodynamically, combining CO_2 and high-energy reactants like H_2 is an ideal strategy to obtain a driving force. As a result, extensive research has been achieved in CO_2 hydrogenation to oxygenates,[5–7] olefins,[8,9] and aromatics.[10,11] Aromatics, as one of the most important chemicals, have enormous market demands for synthetic rubber, polymers, medicines, etc.[12] Considering the hydrogen cost and product market, CO_2-assisted alkane dehydrogenation[13–16] and aromatization[17–19] are other pathways for utilizing CO_2. In these processes, CO_2 usually consumes hydrogen via the reverse water-gas shift reaction to facilitate the conversion of alkanes. As a matter of fact, the carbon atom of CO_2 does not directly participate in the formation of products but is emitted as CO, resulting in a lower atom economy. Although a series of scientific advances have been made toward the reaction mechanism or modification of catalysts,[20–24] the aforementioned constraints still prevent the commercialization of CO_2-based aromatic synthesis techniques. Consequently, exploiting efficient and sustainable CO_2 utilization pathways is a critical challenge.

Methane (CH_4) is not only the principal component of natural gas but is also another, more harmful greenhouse gas. Thus, achieving comprehensive utilization of CH_4 has been a hot topic in research for mitigating the greenhouse effect and advancing the energy revolution. Unfortunately, the high stability of CH_4 limits its transformation and practical application.[25] Methyl halide, which is a versatile platform molecule, can be easily obtained from CH_4 and transformed to chemicals.[26–28] To date, research on the conversion of methyl halide have primarily concentrated on the synthesis of olefins,[29,30] yet less attention has been paid to aromatics. In particular, an approximately 100% CH_3Br conversion and an aromatic yield of 27.9% can be achieved over CuO/ZnO/ZSM–5.[31] Despite some advancement toward metal modification of zeolites[32,33] and route upgrading,[34] the inherent issue is that the imbalance of the H/C ratio between methyl halide and aromatics still limits the aromatics selectivity.

In consideration of the H/C balance between reactants and products, we envision that combining "hydrogen-deficient" species (CO_2) and a "hydrogen-rich" compound (CH_3Cl) would be an ideal strategy to achieve utilization of CO_2 and CH_4. In the present work, we first reported a reaction of CO_2 and CH_3Cl using acidic zeolite catalysts, for which up to 71.3% aromatics selectivity with 100% CH_3Cl conversion can be obtained over H–ZSM–5 at 723 K and 3 MPa. *In situ* Fourier transform infrared spectra and ^{13}C isotope tracer analysis demonstrated that CO_2 can directly involve the formation of aromatics via lactone and cyclopentenone as key intermediates. This work provides an environmental and sustainable pathway for comprehensive utilization of CO_2 and CH_4.

RESULTS

Effect of zeolite topology on the coupling of CO_2 and CH_3Cl to aromatics

To achieve the comprehensive utilization of CO_2 and CH_4, we adopted the "hydrogen-deficient" species (CO_2) and "hydrogen-rich" compound (CH_3Cl) as reactants to synthesis aromatics (Figure 1A). Acidic zeolites were used as catalysts in the coupling reaction, and the effect of zeolite topology on catalytic performance was investigated. The detailed physical properties of all acidic zeolites are shown in Figures S1 and S2 and Table S1. Figure 1B depicts the product selectivities catalyzed by different acidic zeolites under different atmospheres at 3 MPa, 723 K, and 3,000 mL/g_{cat}/h. Obviously, the aromatics selectivity increases to varied extents catalyzed by zeolites with different topologies when CO_2 is introduced to CH_3Cl. Particularly, the aromatics selectivity catalyzed by H–ZSM–5 increases from 54.1% to 71.3%, while alkanes selectivity significantly decreases from 41% to 27.1%. These observations are different from the traditional methyl halide-to-aromatics conversion. Considering that H–ZSM–5 contains no metal, as shown in Table S2, the reverse water-gas shift conversion reaction is difficult to occur. Therefore, we speculate that CO_2 may change the aromatization mechanism. Moreover, the selectivity to aromatics increases by 26.1%, 9.5%, 10.7%, and 4.9% over MCM–22, ZSM–22, ZSM–23, and ZSM–35, respectively. Additionally, SAPO–34, Beta, and Y display low aromatics selectivities with high alkanes selectivities. These results reveal that the acidic zeolites with a 10-membered ring (10MR), especially ZSM–5, are beneficial to produce aromatics in the conversion of CO_2 with CH_3Cl. Therefore, H–ZSM–5 zeolites are adopted as the most efficient catalysts for further investigation. As illustrated in Figure 1C, the product selectivity changes obviously when introducing CO_2 under conditions of 723 K, 0.1 MPa, and 3,000 mL/g_{cat}/h. Aromatics selectivity increases from 16.6% to 28.3% with complete CH_3Cl conversion, whereas the selectivities to olefins and alkanes decrease by 11.1% and 0.5%, respectively. Detailed

[1]National Engineering Research Center of Lower-Carbon Catalysis Technology, Dalian Institute of Chemical Physics, Chinese Academy of Sciences, Dalian 116023, China

[2]University of Chinese Academy of Sciences, Beijing 100049, China

[3]Lead contact

*Correspondence: chliu@dicp.ac.cn (H.L.), wlzhu@dicp.ac.cn (W.Z.)

https://doi.org/10.1016/j.checat.2023.100689

Please cite this article in press as: Fang et al., High carbon utilization for CO_2 conversion with chloromethane to aromatics over acidic zeolite catalyst, Chem Catalysis (2023), https://doi.org/10.1016/j.checat.2023.100689

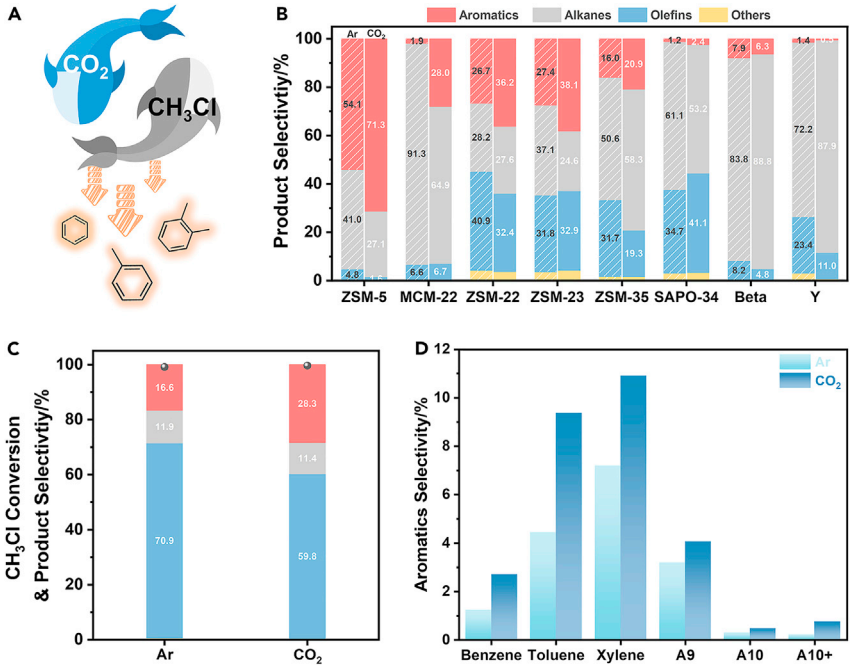

Figure 1. Catalytic performance for the coupling of CO_2 and CH_3Cl over zeolite catalysts with different topologies

(A) The diagram of reaction strategy.

(B) Product selectivity over zeolite catalysts with different topologies under different atmospheres.

(C) CH_3Cl conversion and product selectivity over H–ZSM–5–25 at atmospheric pressure with or without CO_2.

(D) Detailed selectivity of aromatics over H–ZSM–5–25 with Ar versus CO_2 co-feeds at sub-complete CH_3Cl conversion.

Reaction conditions: (B) 723 K, 21 kPa CH_3Cl, (2,580 kPa CO_2, 399 kPa Ar) or (2,979 kPa Ar), 3,000 mL/g_{cat}/h; (C and D) 723 K, 700 Pa CH_3Cl, (86 kPa CO_2, 13.3 kPa Ar) or (99.3 kPa Ar), 3,000 mL/g_{cat}/h. Note that olefins represent $C_2^=$–$C_4^=$, alkanes represent C_1–C_4^0, and others represent C_5+ hydrocarbon excluding aromatics.

aromatics selectivity changes from 1.2% to 2.7% for benzene, 4.4% to 9.4% for toluene, 7.2% to 10.9% for xylene, 3.2% to 4.1% for A9, 0.3% to 0.5% for A10, and 0.2% to 0.7% for A10+, as shown in Figure 1D. Furthermore, the product selectivity exhibits a similar change after cooling down to 623 K under the same conditions (Figure S3). Remarkably, the CH_3Cl conversion dramatically increases from 72.7% to 80.3% after introducing CO_2 versus argon (Ar). These results confirm that even under atmospheric pressure, introducing CO_2 can not only promote the conversion of CH_3Cl but can also change the aromatization mechanism to improve aromatics selectivity.

Effect of SiO_2/Al_2O_3 on the coupling of CO_2 and CH_3Cl to aromatics

The SiO_2/Al_2O_3 of zeolites plays a significant role in acidic catalytic reaction. Furthermore, a series of H–ZSM–5 zeolites have been selected for investigating the effect of SiO_2/Al_2O_3 on the catalytic performance. Figures S4–S6 and Table S1 show the detailed structure properties and chemical information of H–ZSM–5 zeolites with different SiO_2/Al_2O_3. With the increase of SiO_2/Al_2O_3 from 25 to 247, the aromatics selectivity monotonically decreases with complete CH_3Cl conversion under different atmospheres (Figure 2A). Moreover, introducing CO_2 into CH_3Cl conversion, compared with Ar atmosphere, can improve aromatics selectivity and inhibit the formation of alkanes over H–ZSM–5 zeolites with different SiO_2/Al_2O_3. These results

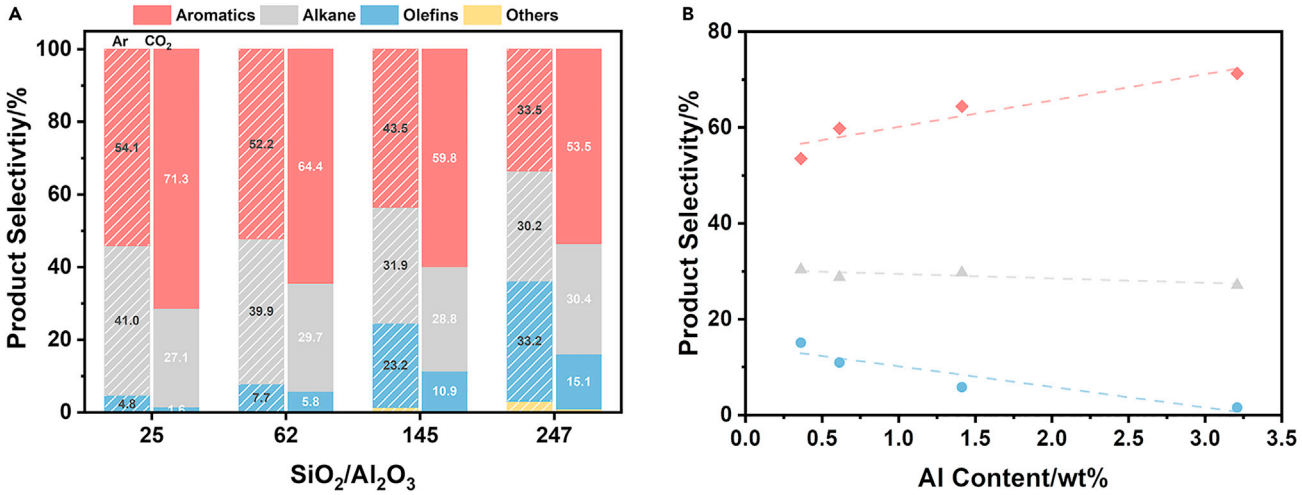

Figure 2. Catalytic performance for the coupling of CO_2 and CH_3Cl over zeolite catalysts with different SiO_2/Al_2O_3 ratios

(A) Product selectivity.

(B) The relationship between product selectivity and Al content of zeolites catalysts.

Reaction conditions: (A) 723 K, 21 kPa CH_3Cl, (2,580 kPa CO_2, 399 kPa Ar) or (2,979 kPa Ar), 3,000 mL/g_{cat}/h; (B) 723 K, 21 kPa CH_3Cl, 2580 kPa CO_2, 399 kPa Ar, 3,000 mL/g_{cat}/h. Note that olefins represent $C_2^{=}$–$C_4^{=}$, alkanes represent C_1–C_4^0, and others represent C_{5+} hydrocarbon excluding aromatics.

indicate that the coupling conversion of CO_2 and CH_3Cl to aromatics is a typical acidic catalytic reaction and that low SiO_2/Al_2O_3 is beneficial for the production of aromatics. Furthermore, the relationship between Al content and product selectivity under different atmospheres is illustrated in Figures 2B and S7. It can be observed that with increasing Al content, aromatics selectivity and alkanes selectivity simultaneously increase, while the selectivity to olefins significantly decreases in Ar atmosphere (Figure S7). These observations are consistent with the traditional mechanism of the hydrogen transfer reaction.[35] Interestingly, introducing CO_2 into CH_3Cl conversion obviously changes the relationship between the Al content and product selectivity (Figure 2B). Compared with the selectivity to aromatics, alkanes and olefins selectivities monotonically decrease with increasing Al content. Therefore, we preliminarily infer that introducing CO_2 into CH_3Cl conversion changes the aromatization mechanism.

Effect of reaction conditions on the coupling of CO_2 and CH_3Cl to aromatics

Figure 3A displays that the variation on product selectivity with total pressure for the coupling conversion of CO_2 and CH_3Cl. With increasing total pressure, the selectivity to aromatics increases monotonically from 28.3% to 71.3%. In particular, compared with the data under atmospheric pressure, the aromatics selectivity dramatically increases to 63.7%. Note that the balances of carbon and chloride elements are 95.8% and 92.1%, respectively, under conditions of 3 MPa, 723 K, and 3,000 mL/g_{cat}/h after 24 h. These results imply that a higher pressure is beneficial for the production of aromatics under CO_2 atmosphere. Additionally, the significant decrease of olefins selectivity indicates that olefins might be an important intermediate for the formation of aromatics. However, the alkanes selectivity decreases from 30.1% to 26.8% with increasing pressure, which further demonstrates that introducing CO_2 can suppress the hydrogen transfer reaction.

As demonstrated in Figure 3B, reaction temperature has also played an important role on the catalytic performance. The aromatics selectivity first increases from 31.6% to 71.3% with reaction temperature and then decreases to 67.3% at 773 K.

Please cite this article in press as: Fang et al., High carbon utilization for CO_2 conversion with chloromethane to aromatics over acidic zeolite catalyst, Chem Catalysis (2023), https://doi.org/10.1016/j.checat.2023.100689

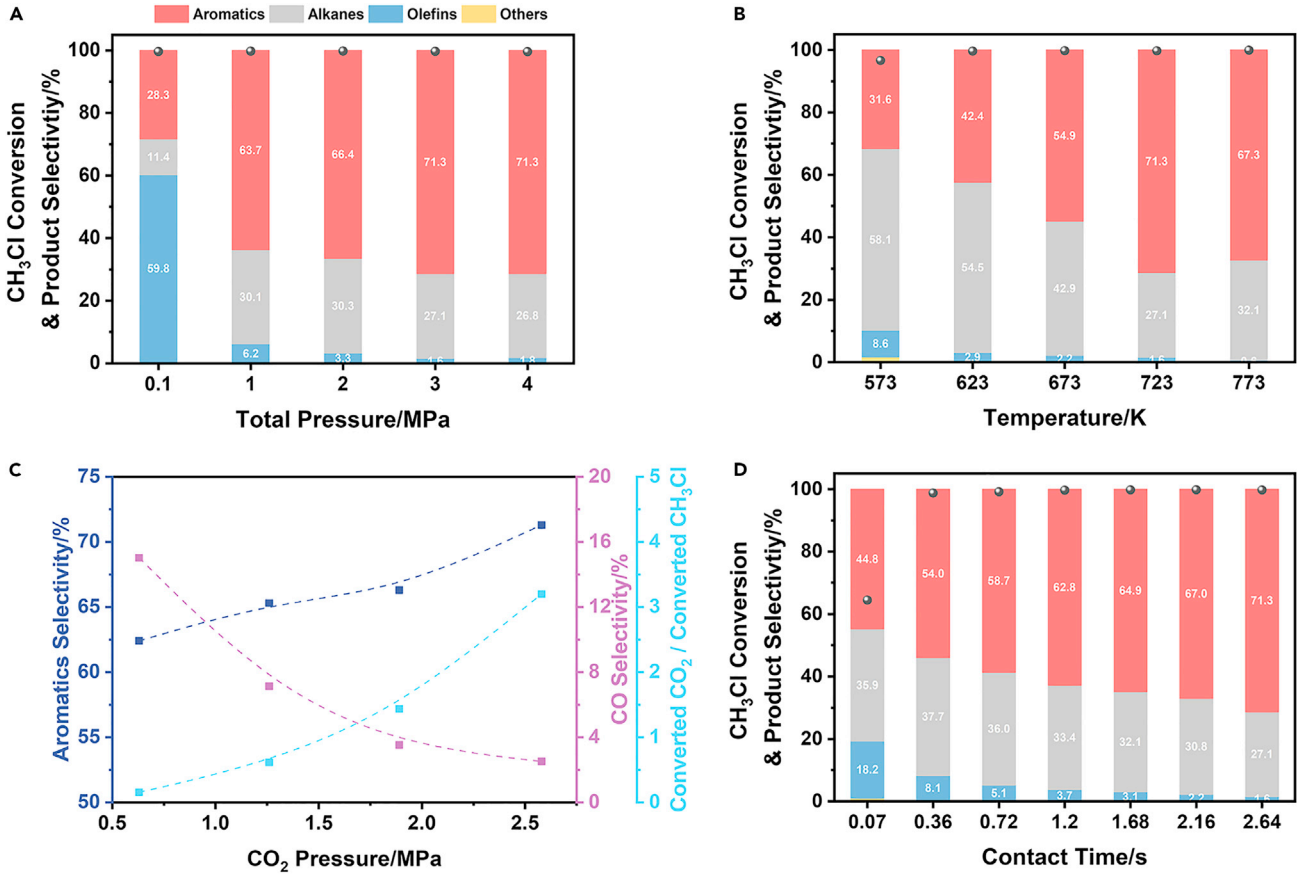

Figure 3. The influence of reaction conditions on the coupling of CO_2 and CH_3Cl over H–ZSM–5–25

(A) The effect of total pressure on CH_3Cl conversion and product selectivity.

(B) The effect of reaction temperature on CH_3Cl conversion and product selectivity.

(C) The effect of CO_2 partial pressure on aromatics selectivity, CO selectivity, and CO_2 conversion.

(D) The effect of contact time on CH_3Cl conversion and product selectivity.

Reaction conditions: (A) 723 K, 3,000 mL/g_{cat}/h, CH_3Cl: CO_2 = 1:120 (mole ratio), Ar as balance gas; (B) 21 kPa CH_3Cl, 2,580 kPa CO_2, 399 kPa Ar, 3,000 mL/g_{cat}/h; (C) 723 K, 21 kPa CH_3Cl, 0–2,580 kPa CO_2, 3,000 mL/g_{cat}/h, Ar as balance gas; (D) 723 K, 21 kPa CH_3Cl, 2,580 kPa CO_2, 399 kPa Ar. Note that olefins represent $C_2^{=}$–$C_4^{=}$, alkanes represent C_1–C_4^0, and others represent C_{5+} hydrocarbon excluding aromatics.

Nevertheless, the change of alkanes selectivity is opposite to that of aromatics with increasing reaction temperature. The minimum selectivity to alkanes is around 27.1% at 723 K, along with the highest selectivity of aromatics. Furthermore, the effect of reaction temperature at atmospheric pressure is shown in Figure S8. Olefins are the main product, which might be due to the occurrence of chloromethane-to-olefin conversion at 0.1 MPa. Specifically, the selectivity to olefins first increases and then declines, reaching up to 59.8% at 723 K. Moreover, the CH_3Cl conversion increases gradually with increasing reaction temperature, revealing that a higher reaction temperature is beneficial for the conversion of CH_3Cl. Although the aromatics selectivity changes slightly, the change trend of aromatics and alkanes is similar to the high-pressure data. Therefore, we deduce that olefins are a key intermediate species for the coupling conversion of CH_3Cl and CO_2 to aromatics.

The data obtained over H–ZSM–5–25 under different CO_2 partial pressures are exhibited in Figure 3C. It is observed that the aromatics selectivity increases monotonically with increasing CO_2 pressure. These results reveal that the aromatics selectivity and CO_2 partial pressure show a positive correlation similar to the coupling

conversion of CO and small molecules.[36–38] We further correlate the ratio of the converted CO_2 to converted CH_3Cl and CO_2 partial pressure. Obviously, with increasing CO_2 partial pressure, the ratio of converted CO_2 to converted CH_3Cl increases monotonically. Thereinto, the CH_3Cl conversion is close to 100%. These results demonstrate that a higher CO_2 partial pressure is beneficial for the conversion of CO_2. Moreover, the CO selectivity declines from 15% to 2.5% with the increase of CO_2 partial pressure. This also means that more CO_2 is converted into aromatics. Therefore, we conclude that an obvious coupling effect exists between CO_2 and CH_3Cl. Additionally, the effect of CH_3Cl partial pressure on the product selectivity is displayed in Figure S9. Obviously, with increasing CH_3Cl partial pressure, the selectivity to aromatics decreases from 73.8% to 71.3%. Moreover, the selectivity to alkanes gradually increases. In fact, the increase of CH_3Cl pressure means the decrease of the ratio of CO_2 to CH_3Cl, which can enhance the hydrogen transfer reactions. In other words, a higher ratio of CO_2 to CH_3Cl is beneficial for the improvement of aromatics selectivity. In summary, the importance of CO_2 in improving aromatics selectivity is further confirmed.

Figure 3D exhibits the effect of contact time on product selectivity and CH_3Cl conversion. With the decrease of contact time, the olefins and alkanes selectivities increase monotonically, while the selectivity to aromatics decreases gradually. These results indicate that the improvement of aromatics selectivity might be caused by the conversion of olefins. After optimizing the reaction conditions, we carried out a stability test under reaction conditions of 3 MPa, 723 K, and 3,000 mL/g_{cat}/h catalyzed by H–ZSM–5–25 (Figure S10). It can be observed that the aromatics selectivity maintains at around 70% with ca. 50% BTX selectivity during 100 h.

The capture and identification of key intermediates during the coupling conversion of CO_2 and CH_3Cl

To clarify the aromatization mechanism during the coupling conversion of CO_2 and CH_3Cl, we captured and identified key intermediate species. The retained species trapped in H–ZSM–5 have been captured via liquid nitrogen cooling at different reaction temperatures (398–773 K) and analyzed by gas chromatography-mass spectrometry (GC–MS) (Figures 4A and 4B). Considerable oxygenated compounds are observed over spent H–ZSM–5–25, consisting of lactone and cyclopentenone species. When the temperature is lower than 448 K, the oxygenates are mainly lactone species with a small number of monocyclic aromatics. With increasing temperature, the lactone species gradually decrease and disappear. Moreover, methyl cyclopentenone appears at 423 K and then increases gradually. Upon further increase of the reaction temperature, cyclopentenone decreased and disappeared at 773 K. Additionally, cycloalkadienes are observed at different temperatures and are considered the key intermediates in the hydrogen transfer reaction. Moreover, a considerable number of aromatics can be observed, which is consistent with the previous results. Additionally, Figure S11 displays a heavy retained species in H–ZSM–5–25. With increasing temperature, the heavy retained species increases, indicating that high temperature can promote the condensation reaction of aromatics. These results demonstrate that lactone and cyclopentenone species are the crucial intermediates during the coupling conversion of CO_2 and CH_3Cl.

Furthermore, we analyzed the change of oxygenated compound using the area of C_2Cl_6 as an internal standard. As illustrated in Figure 4C, the amount of lactone, cyclopentenone, and cycloalkadiene species first increased and then decreased with increasing reaction temperature. Remarkably, the highest values occurred at

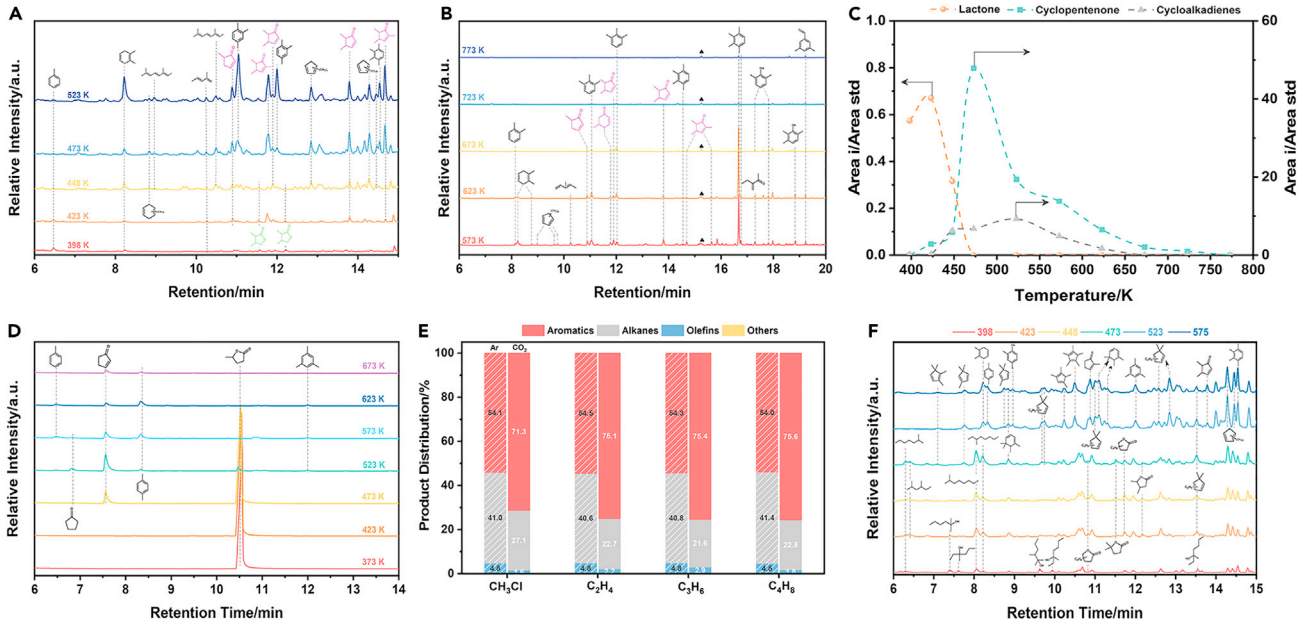

Figure 4. The capture and identification of key intermediate species during the coupling of CO_2 and CH_3Cl to aromatics

(A) GC-MS chromatograms of retained species trapped in zeolite at different reaction temperatures (398–523 K).

(B) GC-MS chromatograms of retained species trapped in zeolite at different reaction temperatures (573–773 K).

(C) The area ratio of lactone/cyclopentenone/cycloalkadienes to C_2Cl_6 on the spent catalyst at different temperatures.

(D) GC-MS chromatograms of carbonaceous species retained in spent H-ZSM-5-25 at different reaction temperatures with γ-valerolactone as ingredient.

Reaction conditions: (A–C) 21 kPa CH_3Cl, 2,580 kPa CO_2, 399 kPa Ar, 3,000 mL/g_{cat}/h, H-ZSM-5-25; (D) 20 mL/min N_2 as carrier gas at STP, 0.2 g H-ZSM-5-25, 0.1 MPa; (E) 3 MPa, 723 K, 3,000 mL/g_{cat}/h, H-ZSM-5-25, Ar as balance gas (note that the number of carbon moles in the feeding remains the same with CH_3Cl); (F) 7 kPa C_3H_6, 2,993 kPa (Ar+CO_2), 3,000 mL/g_{cat}/h, Ar as balance gas.

different temperatures, in order of lactone < cyclopentenone < cycloalkadienes. These results suggest that the above species might have mutual transformation relationship. We deduce that lactone might be converted to cyclopentenone and then be converted to cycloalkadienes. Thereinto, it is reported that cyclopentenone can be transformed into cycloalkadienes.[39] Thus, the correlation between lactone and cyclopentenone should be investigated further. As shown in Figure 4D, the conversion of γ-valerolactone is conducted at different temperatures, and the retained species trapped in H–ZSM–5 are analyzed by GC-MS. With increasing reaction temperature, the amount of γ-valerolactone decreases, implying that γ-valerolactone is converted to product. Moreover, it can be found that cyclopentenone appears at 473 K, exhibiting first increases and then decreases. Additionally, toluene, xylene, and trimethylbenzene appear at 573 K and then increase gradually with the reaction temperature. The above results confirm that γ-valerolactone can be converted to cyclopentenone and then synthesize aromatics.

During the investigation of reaction conditions, we found that olefins are an important intermediate species for the formation of aromatics. Therefore, whether there is a correlation between olefins and γ-valerolactone deserves attention. Different olefins, including ethylene, propylene, and 1-butene, are employed to investigate the role of olefins. As depicted in Figure S12, the olefins are less converted to product under atmospheric pressure, but introducing CO_2 can enhance the aromatization reaction using different olefins. The product distributions with CH_3Cl or olefins feeding are similar to each other at 3 MPa, as shown in Figure 4E. Similarly, the role of

Please cite this article in press as: Fang et al., High carbon utilization for CO_2 conversion with chloromethane to aromatics over acidic zeolite catalyst, Chem Catalysis (2023), https://doi.org/10.1016/j.checat.2023.100689

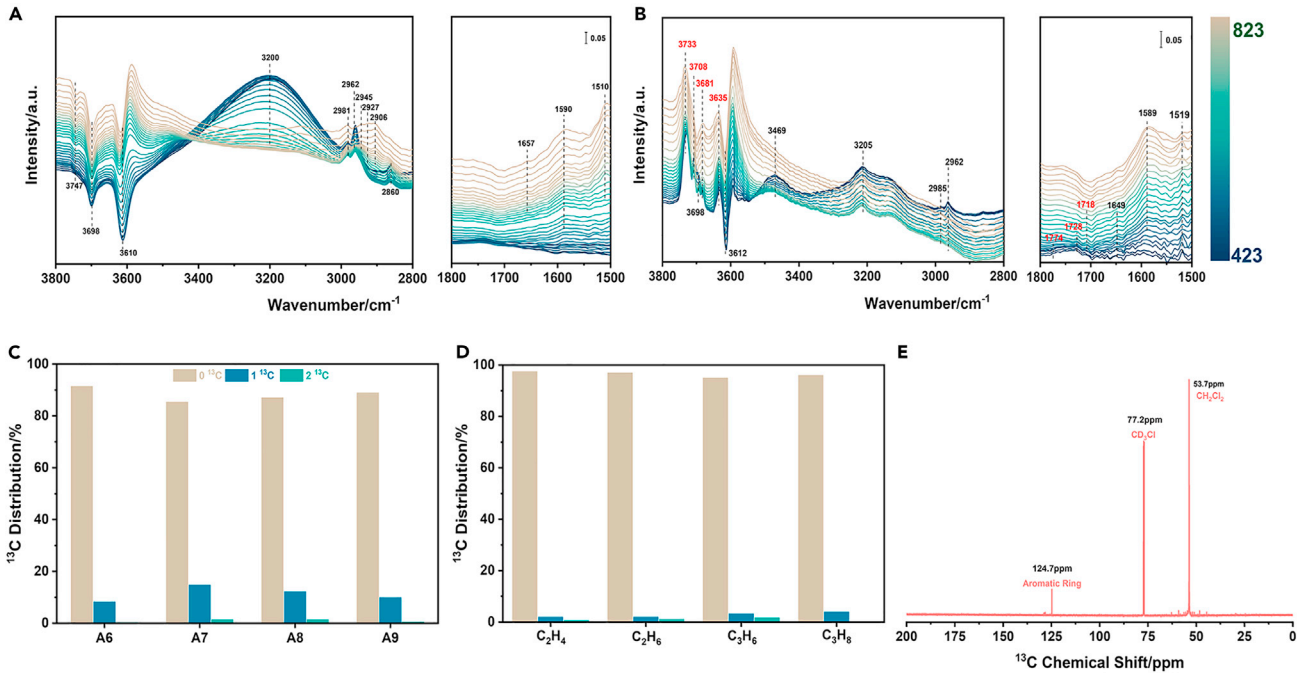

Figure 5. Characterization of reaction mechanism for the coupling conversion of CO_2 and CH_3Cl to aromatics

(A) *In situ* DRIFT spectra in the conversion of CH_3Cl without CO_2 over H–ZSM–5–25.

(B) *In situ* DRIFT spectra in the coupling conversion of CO_2 and CH_3Cl over H–ZSM–5–25.

(C) ^{13}C distribution of aromatics products.

(D) ^{13}C distribution of light alkanes and olefins.

(E) ^{13}C liquid-state NMR spectra of product collected during the coupling of $^{13}CO_2$ and CH_3Cl over H–ZSM–5–25.

Reaction conditions: (A) 700 Pa CH_3Cl, 99.3 kPa Ar, 6,000 mL/g_{cat}/h, Ar as balance gas; (B) 700 Pa CH_3Cl, 99.3 kPa (Ar+CO_2), 6,000 mL/g_{cat}/h, Ar as balance gas; (C–E) 723 K, 3.6 kPa CH_3Cl, 496.4 kPa (Ar+CO_2), 3,150 mL/g_{cat}/h, Ar as balance gas.

CO_2 in enhancing aromatics selectivity can be further confirmed. These results also demonstrated that olefins can be coupled with CO_2 in some way. Afterward, we analyze the residual species trapped in H–ZSM–5–25 for the coupling conversion of C_3H_6 and CO_2 at different temperatures by GC-MS (Figure 4F). It can be found that lactone species exists at low temperatures, exhibiting a volcanic trend. With increasing reaction temperature, the cyclopentenone species appear and increase. Moreover, a considerable number of aromatics can be observed. These results corroborate that olefins can be coupled to form lactone species and then be converted to cyclopentenone species.

Reaction mechanism

To further verify the reaction mechanism, *in situ* diffuse reflectance infrared Fourier transform (DRIFT) and ^{13}C isotope-labeling experiments were conducted. Figure 5A shows the evolution of surface species over H–ZSM–5–25 for the CH_3Cl conversion in Ar atmosphere. Obviously, negative peaks at 3,610, 3,698, and 3,747 cm^{-1} are observed and are assigned to the adsorption of CH_3Cl on hydroxyl groups of H–ZSM–5–25. A wide peak at 3,210 cm^{-1} exists at low temperature and then decreases with temperature, which is attributed to the physical adsorption of CH_3Cl.[40] According to the previous work,[29] the peaks at 2,800–3,000 cm^{-1} are assigned to the surface methoxy groups, resulting from the dissociation adsorption of CH_3Cl on Brønsted acidic sites (BASs). These observations suggest that CH_3Cl is first absorbed on BASs to form methoxy groups. Moreover, the bands at 1,657, 1,590, and 1,510 cm^{-1}, which are attributed to the C=C of olefins, cycloalkadienes,

and aromatics,[41] respectively, appear and then increase with temperature. These observations are consistent with the traditional hydrogen transfer reaction. Remarkably, some new peaks can be observed after introducing CO_2 into CH_3Cl conversion, as exhibited in Figures 5B and S13. The peaks in the range of 3,600~3,750 and 2,200~2,400 cm^{-1} can be correlated with the adsorption of CO_2 according to the standard infrared (IR) spectra of CO_2 (Figure S14). Note that the peaks in the range of 2,100~2,200 cm^{-1}, which are assigned to CO, have not been observed. These results also suggest that CO_2 might directly participate in the conversion of CH_3Cl rather than via reverse water-gas shift reaction. Additionally, the new peaks at 1,774, 1,728, and 1,718 cm^{-1} appear after introducing CO_2, assigned to the C=O bands of ester, lactone, and ketone,[42,43] respectively. Although the intensity of the above peaks is relatively low due to the weakened coupling effect of CO_2 and CH_3Cl under atmospheric pressure, the change trend of spectra is obviously different from that under Ar atmosphere. Specifically, the above peaks attributed to the C=O bond mainly appear at low temperature, then decrease with temperature and vanish. These observations directly confirm that CO_2 can be coupled with CH_3Cl via the formation of an ester group and a ketone group. Furthermore, the intensities of 1,510 and 1,590 cm^{-1} extracted from spectra were compared in CO_2 or Ar atmosphere, as illustrated in Figure S15. After introducing CO_2, the absolute intensities of 1,510 and 1,590 cm^{-1} exhibit a consistent rate of growth. These results might be due to the formation of a large number of oxygen-containing intermediates after introducing CO_2, which obviously promoted the formation of diene species. Therefore, we also demonstrate that the introduction of CO_2 can promote CH_3Cl conversion.

To directly confirm whether CO_2 takes part in the formation of aromatics, a ^{13}C isotope-labeling experiment was conducted. Figures 4C and 4D display the ^{13}C distribution of representative products analyzed by online GC-MS during the coupling conversion of $^{13}CO_2$ and CH_3Cl to aromatics. Moreover, the results of GC are shown in Figure S16. It can be observed that all of the aromatics contain a ^{13}C atom, suggesting that CO_2 takes part in the formation of aromatics. Additionally, the light alkanes and olefins hardly contain a ^{13}C atom. If the aromatization mechanism follows the hydrogen transfer reaction, the ^{13}C distribution of aromatics and light olefins should be consistent. Nevertheless, the amount of ^{13}C in aromatics is obviously higher than light olefins, demonstrating that another pathway to synthesize aromatics exists. Based on our previous results, we deduce that $^{13}CO_2$ can be coupled with olefins without a ^{13}C atom to aromatics via oxygenated compounds. To further validate that whether CO_2 participates in the formation of an aromatic ring, the products collected by CH_2Cl_2 were analyzed by ^{13}C NMR. Figure 5E shows a typical peak at 124.7 ppm, assigned to the C atom at the aromatic ring. These results directly confirmed that CO_2 can be coupled to aromatic rings.

Based on above results, we proposed an aromatization mechanism for the coupling conversion of CO_2 and CH_3Cl to aromatics (Figure 6). CH_3Cl first absorbs on the BAS of H–ZSM–5 to form a surface methoxy group and HCl. The methoxy group can be converted to olefins via hydrocarbon pool mechanism. On the one hand, olefins can be transformed into aromatics via hydrogen transfer reaction. More importantly, there is another pathway to form aromatics, including the coupling of CO_2 and olefins to lactone species and then converting to cyclopentenone species. Finally, the cyclopentenone further converts into aromatics via dehydration and methylation reactions. This route efficiently suppressed the hydrogen transfer reaction to improve aromatics selectivity to a great extent.

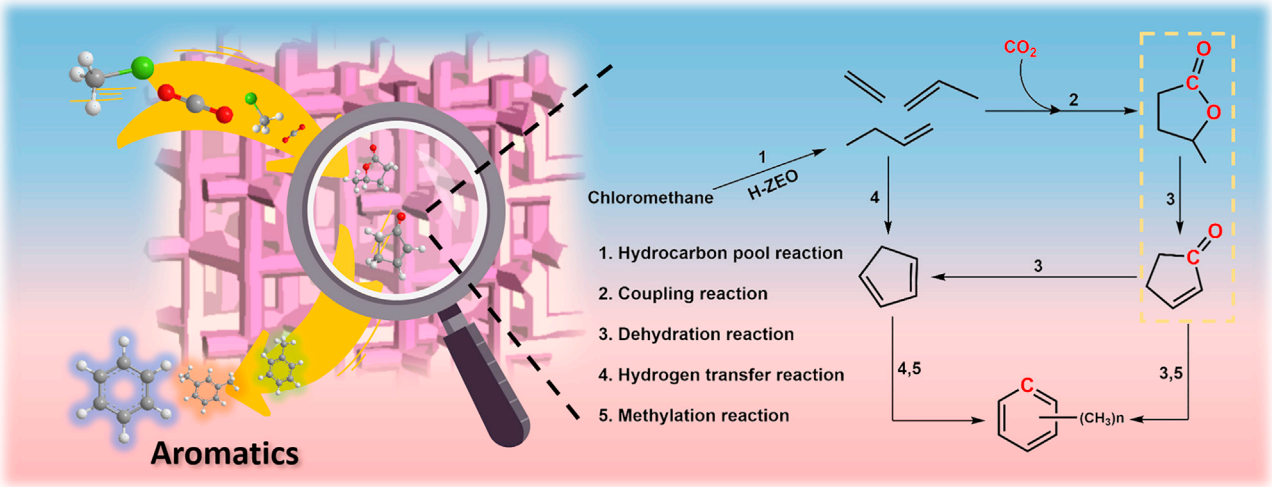

Figure 6. The proposed reaction mechanism for the coupling of CO_2 and CH_3Cl to aromatics over H–ZSM–5

DISCUSSION

In summary, we first developed an innovative pathway to greenhouse gas utilization for aromatics production. This process is achieved by combination of "hydrogen-deficient" species (CO_2) and a "hydrogen-rich" compound (CH_3Cl) catalyzed by acidic zeolites, especially containing a 10MR. We demonstrated that the presence of CO_2 can not only promote the conversion of CH_3Cl but can also regulate product distribution. High aromatics selectivity (71.3%) and BTX selectivity (~50%) are obtained over H–ZSM–5–25 at 723 K, 3 MPa, and 3,000 mL/g_{cat}/h. Combined with multiple characterizations, lactone and cyclopentenone species are proven to be the key intermediates during the formation of aromatics. More importantly, CO_2 directly incorporates into the aromatics ring via the above intermediates rather than through reverse water-gas shift reaction. This investigation provides an attractive and promising route to simultaneously achieve the comprehensive utilization of CO_2 and CH_4.

EXPERIMENTAL PROCEDURES

Resource availability

Lead contact

Further information and requests for resources should be directed to and will be fulfilled by the lead contact, Wenliang Zhu (wlzhu@dicp.ac.cn).

Materials availability

This study did not generate new materials.

Data and code availability

This study did not generate any datasets.

Catalyst information

The H–ZSM–5 with different SiO_2/Al_2O_3 was purchased from Naikai University Catalyst Company. The samples were named as H–ZSM–5–X. Thereinto, X represents the ratio of SiO_2/Al_2O_3. The other zeolites with different topologies were also obtained from commercial suppliers.

Catalyst characterization

The crystallinity of zeolites was characterized by PANalytical X'Pert PRO powder X-ray diffraction (XRD) using a Cu-Kα (λ = 0.151 nm) radiation source operated at 40 kV and 40 mA. The bulk composition of zeolites was determined by Philips Magix-601 X-ray fluorescence (XRF). The surface morphology images of zeolites were obtained by Hitachi SU8020 scanning electron microscopy (SEM). The textural properties of zeolites with different topologies were obtained from N_2 adsorption and desorption at 77 K. Before the measurement, the samples were degassed at 523 K to remove the water in zeolites under vacuum for 1 h. The surface area of samples was estimated by the Brunauer-Emmett-Teller (BET) model. The pore volumes of samples were calculated by the t-plot method. The acidity of zeolites was measured on a Micromeritics Auto Chem 2920 equipped with a thermal conductivity detector (TCD). In brief, 0.15 g zeolite sample was loaded into a U-shaped quartz tube and pretreated at 823 K for 30 min in helium. Then, the sample was cooled to 423 K and saturated with NH_3. After removing the physically adsorbed NH_3 in helium, desorption was performed from 423 to 923 K at a heating rate of 10 K/min in He gas. The ^{13}C liquid nuclear magnetic resonance (NMR) spectra of products were obtained using a Bruker Avance III HD 700 MHz spectrometer with a 9.40 T wide-bore magnet. The resonance frequencies were set up at 176 MHz for ^{13}C. In a 10 mm NMR tube, 0.15 mL $CDCl_3$ was dissolved in 0.5 mL samples. ^{13}C NMR spectra were recorded using high-power proton decoupling. Fixed scans were collected with a $\pi/2$ pulse of 12.6 μs and a 2 s recycle delay.

In situ DRIFT spectra were carried out on a Bruker Tensor 27 instrument equipped with a diffuse reflectance attachment and a mercury cadmium telluride (MCT) detector under reaction conditions. Firstly, 50 mg H–ZSM–5–25 was placed in the diffuse reflectance IR cell, and then the sample was calcined in the N_2 stream at 723 K for 2 h. Afterward, the catalyst was cooled down to reaction temperature in the N_2 stream, and the spectrum of the sample was recorded as background. The stream of mixed gas (0.7% CH_3Cl, 86% CO_2, 13.3% Ar) or (0.7% CH_3Cl, 99.3% Ar) at 10 mL/min was introduced into the cell at 0.1 MPa. The spectra were scanned continuously to observe surface species. The *in situ* DRIFT spectra of the coupling of propene and CO_2 were carried out with (0.5% C_3H_6, 49.5% CO_2, 50% Ar) or (0.5% CH_3Cl, 99.5% Ar) at 10 mL/min under atmospheric pressure.

To capture and identify the key intermediate for the coupling conversion of CO_2 and CH_3Cl, the catalysts were collected after reaction. The spent zeolites were dissolved within 20% HF solution and extracted by CH_2Cl_2, then analyzed via GC-MS (Agilent 7890/5975C). Furthermore, we carried out the ^{13}C isotope-tracing experiments. H–ZSM–5–25 in the amount of 0.2 g was put into the reactor. The catalyst was first pretreated at 723 K for 3 h with argon gas flow (flow rate, 20 mL/min), and the temperature was maintained at 723 K. The mixed gas (CO_2/CH_3Cl = 120) was introduced into the reactor in the presence of $^{13}CO_2$ or $^{12}CO_2$. The products were analyzed by online GC-MS. Additionally, the products were collected by CH_2Cl_2 for 10 min and analyzed by ^{13}C liquid-state NMR.

Catalyst test

The coupling conversion of CO_2 and CH_3Cl to aromatics was performed in a high-pressure fixed-bed flow reactor (inside diameter = 7 mm) made by stainless steel. Typically, a proper amount of the catalyst (20–40 mesh) mixed with quartz sand (20–40 mesh) was loaded into the reactor. Prior to reaction, the catalyst was first pretreated at 723 K for 3 h with argon gas flow (flow rate, 40 mL/min) to remove water in the zeolite and reactor. Subsequently, the temperature was maintained at 723 K. The

reactants that contained CH_3Cl and CO_2 were introduced into the reactor at a fixed pressure, where argon gas was the balance gas. In doing so, the results of the catalyst evaluation were discussed using the data at equilibrium.

Products were analyzed by online gas chromatographs (Agilent 7890A), which were equipped with a flame ionization detector (FID) and a TCD. The PLOT-Q capillary column was connected with the FID to separate and analyze the products. The TDX-1 packing column was connected with the TCD to separate and analyze CO/CO_2/Ar/CH_4. The CH_3Cl conversion and products selectivity were calculated on a molar carbon basis:

$$\text{Conv } CH_3Cl = \frac{\sum_1^n nC_nH_m - CH_3Cl_{outlet}}{\sum_1^n nC_nH_m} \times 100\% \text{ and}$$

$$\text{Sel product X} = \frac{\text{products } X_{outlet}}{\sum_1^n nC_nH_m - CH_3Cl_{outlet}} \times 100\%,$$

where nC_nH_m is the carbon atoms of all C_nH_m at the outlet, CH_3Cl_{outlet} is the carbon atoms of CH_3Cl at the outlet, and product X_{outlet} is the carbon atoms of product X at the outlet.

$$\text{Conv } CO_2 = \frac{CO_{2inlet} - CO_{2outlet}}{CO_{2inlet}} \times 100\%$$

$$\text{Sel CO} = \frac{CO_{outlet}}{CO_{2inlet} - CO_{2outlet}} \times 100\%$$

CO_{2inlet} is the moles of CO_2 at the inlet, and $CO_{2outlet}$ is the moles of CO_2 at the outlet.

SUPPLEMENTAL INFORMATION

Supplemental information can be found online at https://doi.org/10.1016/j.checat.2023.100689.

ACKNOWLEDGMENTS

This work was supported by the National Natural Science Foundation of China (grant nos. 21972141, 21991094, and 21991090); the "Transformational Technologies for Clean Energy and Demonstration," Strategic Priority Research Program of the Chinese Academy of Sciences (grant no. XDA21030100); the Dalian High Level Talent Innovation Support Program (2017RD07); the National Special Support Program for High Level Talents (SQ2019RA2TST0016); the National Key Research and Development Program of China (grant no. 2022YFE0116000); and Youth Innovation Promotion Association CAS (2021182). Finally, Xudong Fang is grateful for the patience, care, and support from Jinqiu Yuan over the past six years. Will you marry me and share our lives together?

AUTHOR CONTRIBUTIONS

Conceptualization, Z.L., W.Z., H.L, and X.F.; investigation, X.F., H.L., B.L., Z.C., M.X., L.Y., and J.H.; validation, X.F. and Z.C.; writing – original draft, X.F.; visualization, X.F. and H.L.; writing – review & editing, Z.L., W.Z., and H.L.; supervision, Z.L., W.Z., and H.L.

DECLARATION OF INTERESTS

The authors declare no competing interests.

INCLUSION AND DIVERSITY

We support inclusive, diverse, and equitable conduct of research.

Received: March 27, 2023
Revised: May 15, 2023
Accepted: June 12, 2023
Published: July 5, 2023

REFERENCES

1. Huang, K., Sun, C.L., and Shi, Z.J. (2011). Transition-metal-catalyzed C-C bond formation through the fixation of carbon dioxide. Chem. Soc. Rev. *40*, 2435–2452. https://doi.org/10.1002/chin.201140250.

2. Sakakura, T., Choi, J.C., and Yasuda, H. (2007). Transformation of Carbon Dioxide. Chem. Rev. *107*, 2365–2387.

3. Tackett, B.M., Gomez, E., and Chen, J.G. (2019). Net reduction of CO2 via its thermocatalytic and electrocatalytic transformation reactions in standard and hybrid processes. Nat. Catal. *2*, 381–386. https://doi.org/10.1038/s41929-019-0266-y.

4. Ye, R.P., Ding, J., Gong, W., Argyle, M.D., Zhong, Q., Wang, Y., Russell, C.K., Xu, Z., Russell, A.G., Li, Q., et al. (2019). CO2 hydrogenation to high-value products via heterogeneous catalysis. Nat. Commun. *10*, 5698. https://doi.org/10.1038/s41467-019-13638-9.

5. Pinheiro Araújo, T., Mondelli, C., Agrachev, M., Zou, T., Willi, P.O., Engel, K.M., Grass, R.N., Stark, W.J., Safonova, O.V., Jeschke, G., et al. (2022). Flame-made ternary Pd-In2O3-ZrO2 catalyst with enhanced oxygen vacancy generation for CO2 hydrogenation to methanol. Nat. Commun. *13*, 5610. https://doi.org/10.1038/s41467-022-33391-w.

6. Zhao, D., Tan, Z., Zhao, H., Fan, F., Chang, S., Jiang, K., Fang, Y., Zhu, C., Liu, X., Tang, Y., et al. (2022). The role of Cu1–O3 species in single-atom Cu/ZrO2 catalyst for CO2 hydrogenation. Opt. Lett. *47*, 818–821. https://doi.org/10.1038/s41929-022-00840-0.

7. Zhou, H., Chen, Z., López, A.V., López, E.D., Lam, E., Tsoukalou, A., Willinger, E., Kuznetsov, D.A., Mance, D., Kierzkowska, A., et al. (2021). Engineering the Cu/Mo2CTx (MXene) interface to drive CO2 hydrogenation to methanol. Nat. Catal. *4*, 860–871. https://doi.org/10.1038/s41929-021-00684-0.

8. Wang, S., Zhang, L., Zhang, W., Wang, P., Qin, Z., Yan, W., Dong, M., Li, J., Wang, J., He, L., et al. (2020). Selective Conversion of CO2 into Propene and Butene. Chem *6*, 3344–3363. https://doi.org/10.1016/j.chempr.2020.09.025.

9. Gao, P., Li, S., Bu, X., Dang, S., Liu, Z., Wang, H., Zhong, L., Qiu, M., Yang, C., Cai, J., et al. (2017). Direct conversion of CO2 into liquid fuels with high selectivity over a bifunctional catalyst. Nat. Chem. *9*, 1019–1024. https://doi.org/10.1038/nchem.2794.

10. Ni, Y., Chen, Z., Fu, Y., Liu, Y., Zhu, W., and Liu, Z. (2018). Selective conversion of CO2 and H2 into aromatics. Nat. Commun. *9*, 3457. https://doi.org/10.1038/s41467-018-05880-4.

11. Li, Z., Qu, Y., Wang, J., Liu, H., Li, M., Miao, S., and Li, C. (2019). Highly Selective Conversion of Carbon Dioxide to Aromatics over Tandem Catalysts. Joule *3*, 570–583. https://doi.org/10.1016/j.joule.2018.10.027.

12. Li, T., Shoinkhorova, T., Gascon, J., and Ruiz-Martínez, J. (2021). Aromatics Production via Methanol-Mediated Transformation Routes. ACS Catal. *11*, 7780–7819. https://doi.org/10.1021/acscatal.1c01422.

13. Biswas, A.N., Xie, Z., and Chen, J.G. (2022). Can CO2-assisted alkane dehydrogenation lead to negative CO2 emissions? Joule *6*, 269–273. https://doi.org/10.1016/j.joule.2021.12.008.

14. Zhang, J.-b., He, H.-h., Tian, H.-F., Liao, J.-K., Zha, F., Guo, X.-J., Tang, X., and Chang, Y. (2021). Coupling of propane with CO2 to propylene over Zn-promoted In/HZSM-5 catalyst. Can. J. Chem. *99*, 619–627. https://doi.org/10.1139/cjc-2020-0495.

15. Gomez, E., Kattel, S., Yan, B., Yao, S., Liu, P., and Chen, J.G. (2018). Combining CO2 reduction with propane oxidative dehydrogenation over bimetallic catalysts. Nat. Commun. *9*, 1398. https://doi.org/10.1038/s41467-018-03793-w.

16. Wang, S., Zhang, L., Wang, P., Liu, X., Chen, Y., Qin, Z., Dong, M., Wang, J., He, L., Olsbye, U., and Fan, W. (2022). Highly effective conversion of CO2 into light olefins abundant in ethene. Chem *8*, 1376–1394. https://doi.org/10.1016/j.chempr.2022.01.004.

17. Ihm, S.K., Park, Y.K., and Lee, S.W. (2000). Effects of CO2 addition on the aromatization of propane over metal-loaded ZSM-5 catalysts. Appl. Organomet. Chem. *14*, 778–782. https://doi.org/10.1002/1099-0739(200012)14:12<778::Aid-aoc75>3.0.Co;2-7.

18. Niu, X., Nie, X., Yang, C., and Chen, J.G. (2020). CO2-Assisted propane aromatization over phosphorus-modified Ga/ZSM-5 catalysts. Catal. Sci. Technol. *10*, 1881–1888. https://doi.org/10.1039/c9cy02589h.

19. Bradford, M.C., Te, M., Konduru, M., and Fuentes, D.X. (2004). CH4–C2H6–CO2 conversion to aromatics over Mo/SiO2/H-ZSM-5. Appl. Catal., A *266*, 55–66. https://doi.org/10.1016/j.apcata.2004.01.026.

20. Wang, D., Xie, Z., Porosoff, M.D., and Chen, J.G. (2021). Recent advances in carbon dioxide hydrogenation to produce olefins and aromatics. Chem *7*, 2277–2311. https://doi.org/10.1016/j.chempr.2021.02.024.

21. Wang, Y., Tan, L., Tan, M., Zhang, P., Fang, Y., Yoneyama, Y., Yang, G., and Tsubaki, N. (2018). Rationally Designing Bifunctional Catalysts as an Efficient Strategy To Boost CO2 Hydrogenation Producing Value-Added Aromatics. ACS Catal. *9*, 895–901. https://doi.org/10.1021/acscatal.8b01344.

22. Ramirez, A., Dutta Chowdhury, A., Dokania, A., Cnudde, P., Caglayan, M., Yarulina, I., Abou-Hamad, E., Gevers, L., Ould-Chikh, S., De Wispelaere, K., et al. (2019). Effect of Zeolite Topology and Reactor Configuration on the Direct Conversion of CO2 to Light Olefins and Aromatics. ACS Catal. *9*, 6320–6334. https://doi.org/10.1021/acscatal.9b01466.

23. Wang, Y., Gao, X., Wu, M., and Tsubaki, N. (2021). Thermocatalytic hydrogenation of CO2 into aromatics by tailor-made catalysts: Recent advancements and perspectives. EcoMat *3*. https://doi.org/10.1002/eom2.12080.

24. Gao, W., Guo, L., Cui, Y., Yang, G., He, Y., Zeng, C., Taguchi, A., Abe, T., Ma, Q., Yoneyama, Y., and Tsubaki, N. (2020). Selective Conversion of CO2 into para-Xylene over a ZnCr2O4-ZSM-5 Catalyst. ChemSusChem *13*, 6541–6545. https://doi.org/10.1002/cssc.202002305.

25. Huang, K., Miller, J.B., Huber, G.W., Dumesic, J.A., and Maravelias, C.T. (2018). A General Framework for the Evaluation of Direct Nonoxidative Methane Conversion Strategies. Joule *2*, 349–365. https://doi.org/10.1016/j.joule.2018.01.001.

26. Lin, R., Amrute, A.P., and Pérez-Ramírez, J. (2017). Halogen-Mediated Conversion of Hydrocarbons to Commodities. Chem. Rev. *117*, 4182–4247. https://doi.org/10.1021/acs.chemrev.6b00551.

27. Zichittella, G., Aellen, N., Paunović, V., Amrute, A.P., and Pérez-Ramírez, J. (2017). Olefins from Natural Gas by Oxychlorination. Angew. Chem. Int. Ed. Engl. *56*, 13670–13674. https://doi.org/10.1002/anie.201706624.

28. Zichittella, G., Paunović, V., and Pérez-Ramírez, J. (2019). Mechanistic Understanding of Halogen-mediated Catalytic Processes for Selective Natural Gas Functionalization. Chimia *73*, 288–293. https://doi.org/10.2533/chimia.2019.288.

29. Jaumain, D., and Su, B.-L. (2003). Direct catalytic conversion of chloromethane to higher hydrocarbons over a series of ZSM-5 zeolites exchanged with alkali cations. J. Mol. Catal. A: Chem. *197*, 263–273. https://doi.org/10.1016/s1381-1169(02)00622-2.

30. Gamero, M., Valle, B., Castaño, P., Aguayo, A.T., and Bilbao, J. (2018). Reaction network of the chloromethane conversion into light olefins using a HZSM-5 zeolite catalyst. J. Ind. Eng.

Chem. *61*, 427–436. https://doi.org/10.1016/j.jiec.2017.12.042.

31. Lorkovic, I.M., Noy, M.L., Schenck, W.A., Belon, C., Weiss, M., Sun, S., Sherman, J.H., McFarland, E.W., Stucky, G.D., and Ford, P.C. (2004). C1 oxidative coupling via bromine activation and tandem catalytic condensation and neutralization over CaO/zeolite composites - II. Product distribution variation and full bromine confinement. Catal. Today *98*, 589–594. https://doi.org/10.1016/j.cattod.2004.09.013.

32. Wang, P., Chen, L., Xie, J., Li, H., Au, C.-T., and Yin, S.-F. (2017). Enhanced catalytic performance in CH3Br conversion to benzene, toluene, and xylene over steamed HZSM-5 zeolites. Catal. Sci. Technol. *7*, 2559–2565. https://doi.org/10.1039/c7cy00334j.

33. Lorkovic, I., Noy, M., Schenck, W., Belon, C., Weiss, M., Sun, S., Sherman, J., Mcfarland, E., Stucky, G., and Ford, P. (2004). C1 oxidative coupling via bromine activation and tandem catalytic condensation and neutralization over CaO/zeolite composites II. Product distribution variation and full bromine confinement. Catal. Today *98*, 589–594.

34. Fang, X., Liu, H., Chen, Z., Liu, Z., Ding, X., Ni, Y., Zhu, W., and Liu, Z. (2022). Highly Enhanced Aromatics Selectivity by Coupling of Chloromethane and Carbon Monoxide over H-ZSM-5. Angew. Chem. Int. Ed. Engl. *61*, e202114953. https://doi.org/10.1002/anie.202114953.

35. Sun, X., Mueller, S., Liu, Y., Shi, H., Haller, G.L., Sanchez-Sanchez, M., van Veen, A.C., and Lercher, J.A. (2014). On reaction pathways in the conversion of methanol to hydrocarbons on HZSM-5. J. Catal. *317*, 185–197. https://doi.org/10.1016/j.jcat.2014.06.017.

36. Wen, F., Zhang, J., Chen, Z., Zhou, Z., Liu, H., Zhu, W., and Liu, Z. (2021). Coupling conversion of methane with carbon monoxide via carbonylation over Zn/HZSM-5 catalysts. Catal. Sci. Technol. *11*, 1358–1364. https://doi.org/10.1039/d0cy01983f.

37. Chen, Z., Ni, Y., Zhi, Y., Wen, F., Zhou, Z., Wei, Y., Zhu, W., and Liu, Z. (2018). Coupling of Methanol and Carbon Monoxide over H-ZSM-5 to Form Aromatics. Angew. Chem. Int. Ed. Engl. *57*, 12549–12553. https://doi.org/10.1002/anie.201807814.

38. Cheung, P., Bhan, A., Sunley, G.J., and Iglesia, E. (2006). Selective carbonylation of dimethyl ether to methyl acetate catalyzed by acidic zeolites. Angew. Chem. Int. Ed. Engl. *45*, 1617–1620. https://doi.org/10.1002/anie.200503898.

39. Liu, Z., Dong, X., Liu, X., and Han, Y. (2016). Oxygen-containing coke species in zeolite-catalyzed conversion of methanol to hydrocarbons. Catal. Sci. Technol. *6*, 8157–8165. https://doi.org/10.1039/c6cy01463a.

40. Wei, Y., Zhang, D., Liu, Z., and Su, B. (2006). Highly efficient catalytic conversion of chloromethane to light olefins over HSAPO-34 as studied by catalytic testing and in situ FTIR. J. Catal. *238*, 46–57. https://doi.org/10.1016/j.jcat.2005.11.021.

41. Wei, C., Li, J., Yang, K., Yu, Q., Zeng, S., and Liu, Z. (2021). Aromatization mechanism of coupling reaction of light alkanes with CO over acidic zeolites: Cyclopentenones as key intermediates. Chem Catal. *1*, 1273–1290. https://doi.org/10.1016/j.checat.2021.09.004.

42. Zhou, J.Y., Lu, G.D., and Wu, S.H. (1992). A New Approach for the Synthesis of α-Methylene-γ-Butyrolactones from α-Bromomethyl Acrylic Acids (or Esters). Synth. Commun. *22*, 481–487.

43. Lievens, C., Mourant, D., He, M., Gunawan, R., Li, X., and Li, C.-Z. (2011). An FT-IR spectroscopic study of carbonyl functionalities in bio-oils. Fuel *90*, 3417–3423. https://doi.org/10.1016/j.fuel.2011.06.001.